

# Simulation-based Approach for Fast Optimal Control of a Stefan Problem with Application to Cell Therapy

Prakitr Srisuma<sup>a</sup>, George Barbastathis<sup>a</sup>, Richard D. Braatz<sup>a</sup>

<sup>a</sup>Massachusetts Institute of Technology, Cambridge, MA 02139, USA

---

## Abstract

This article describes a new, efficient way of finding control and state trajectories in optimal control problems by transformation into a system of differential-algebraic equations (DAEs). The optimal control and state vectors can be obtained via simulation of the resulting DAE system with the selected DAE solver, eliminating the need for an optimization solver. Our simulation-based framework was demonstrated and benchmarked against various optimization-based approaches via four case studies associated with optimization and control of a Stefan problem with application to cell therapy. The simulation-based approach is faster than every optimization-based method by more than an order of magnitude while giving the same level of accuracy in all cases. The proposed technique offers an efficient and reliable framework for optimal control, serving as a promising alternative to the traditional techniques in applications where speed is crucial, e.g., real-time online model predictive control.

*Key words:* Optimal Control, Differential-Algebraic Equations, Stefan Problem, Moving Boundary, Cell Therapy

---

## 1 Introduction

A Stefan problem describes the evolution of a moving interface during phase change, e.g., freezing and melting (Carslaw and Jaeger, 1959; Bird et al., 2002). Different Stefan problem formulations have been applied to study various industrial and natural systems, including polymorphous materials (Tao, 1979), steel casting (Hill and Wu, 1994; Petrus et al., 2010), biological tissue (Rabin and Shitzer, 1995, 1997), alloy formation (Brosa Planella et al., 2019, 2021), glaciation (Mikova et al., 2017), phase change materials (Brezina et al., 2018), cryopreservation (Dalwadi et al., 2020), and cell therapy (Srisuma et al., 2023b). Numerical techniques have been developed for implementing and simulating the Stefan problems (Meyer, 1971; Velardi and Barresi, 2008; Kurbatova and Ermolaeva, 2019; Gusev et al., 2021; Srisuma et al., 2023b).

Optimal control of Stefan problems was extensively investigated and proven useful for various industrial applications over the past few decades, with many different objective functions, constraints, and controls (manipulated variables) considered. Some examples are the control of the heating process to satisfy the heating speed and thermoelastic stress constraints by manipulating the furnace temperature (Roubíček, 1986), the stabilization of the moving boundary and temperature/concentration

fields by varying the heat flux (Pawlow, 1987), the maximization of the amount of melted solid in the melting process via controlling the heat flux (Silva Neto and White, 1994), the control of the moving boundary to follow the desired path in the solidification process by manipulating the wall temperature (Hinze and Ziegenbalg, 2007), the control of the water level in the drainage basin by varying the discharge velocity (Miyaoka and Kawahara, 2008), the optimization of a thin-film drying process via manipulating the air temperature (Mesbah et al., 2014), and the minimization of the metallurgical length (ML) deviation in steel casting via controlling the boundary heat flux (Chen et al., 2019).

All the aforementioned studies rely on optimization algorithms/solvers to obtain the optimal control trajectories. The widely used approach is to replace the time-varying control vector by a finite-dimensional parameterization (e.g., a spline) and carry out numerical discretization to transform the dynamic optimization into a nonlinear algebraic program (Kishida et al., 2013; Scott et al., 2018; Nolasco et al., 2021, for example). This overall approach has many variations, including methods that sequentially switch between solving the numerical discretization of the underlying partial differential-algebraic equations (PDAEs) and running an algebraic optimizer, or simultaneously solving a single large sparse optimization with the numerical discretization equations as explicit constraints (Neuman and Sen, 1974; Tsang et al., 1975; Mellefont and Sargent, 1978; Sargent and Sullivan, 1978; Biegler, 2007; Nolasco et al., 2021). Numerous optimal control algorithms have been developed for efficient solutions to facilitate real-time applications such as model predictive control (e.g., see detailed discussions by Rodrigues et al. (2014) and Nolasco et al. (2021)). Alternatively, Berliner et al. (2022) showed that it is pos-

---

*Email addresses:* prakitr@mit.edu (Prakitr Srisuma), gbarb@mit.edu (George Barbastathis), braatz@mit.edu (Richard D. Braatz).

<sup>1</sup> Corresponding author: Richard D. Braatz

<sup>2</sup> This manuscript is an extension of a paper published in the Proceedings of the American Control Conference (Srisuma et al., 2024).

arXiv:2412.18272v1 [eess.SY] 24 Dec 2024

sible to reformulate some optimal control problems as a mixed continuous-discrete system of index-1 PDAEs. The PDAE system is then solved numerically by feeding the differential-algebraic equations (DAEs) obtained by spatial discretization into a DAE solver. In this approach, the optimal control vector is obtained directly by a DAE solver, without using any optimization solver, resulting in a highly computationally efficient solution to the optimal control problem. Recently, this approach was used to solve optimal control problems associated with a Stefan problem (Srisuma et al., 2024).

Although optimal control with Stefan problems has been explored for a wide range of processes, applications to cell therapy have not been available. Previous studies showed that accurate prediction, control, and optimization of cryopreservation and cell thawing can improve the viability and quality of the resulting cells, which directly benefits cell therapy (Seki and Mazur, 2008; Jang et al., 2017; Baboo et al., 2019; Hunt, 2019; Bojic et al., 2021; Cottle et al., 2022; Uhrig et al., 2022). These benefits and case studies therefore motivate the development of an efficient Stefan problem-based optimal control algorithm for cell therapy.

This article describes an optimal control algorithm via DAE reformulation and simulation, referred to as the simulation-based approach, for cell therapy applications. The main contributions of this work are to

- (1) derive the simulation-based approach for optimal control of a Stefan problem for the cell thawing process in cell therapy;
- (2) generalize the simulation-based approach for both index-1 and high-index DAE systems;
- (3) demonstrate and benchmark the simulation-based algorithm against various optimization-based optimal control algorithms; and
- (4) apply the proposed approach to efficiently and accurately solve several practical problems associated with optimization and control of cell thawing.

This article is organized as follows. Section 2 describes the cell thawing system and summarizes the mechanistic model and equations. Section 3 discusses various techniques for solving optimal control problems and introduces the simulation-based approach. Section 4 demonstrates the simulation-based approach via case studies. Finally, Section 5 summarizes the study.

## 2 Stefan Problem and Cell Thawing

The system used for the demonstration of our optimal control technique in this article concerns cell thawing, which is a process used in cell therapy before cells are introduced to the patients (Fig. 1). During thawing, energy is continuously supplied by a heater to thaw the material in a vial. A mechanistic model of cell thawing can be formulated as a Stefan problem (Srisuma et al., 2023b). Heat transfer in the solid and liquid domains can be described by the energy balance equation,

$$\frac{1}{\alpha} \frac{\partial T}{\partial t} = \frac{\partial^2 T}{\partial r^2} + \frac{1}{r} \frac{\partial T}{\partial r}, \quad (1)$$

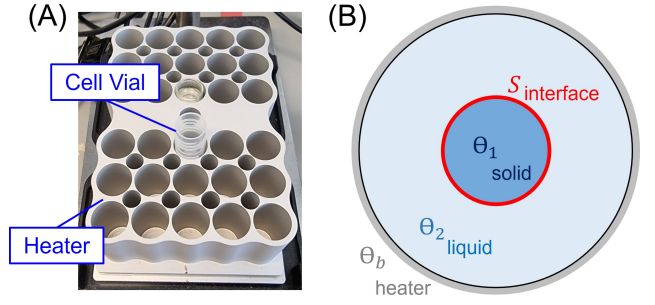


Fig. 1. (A) In cell thawing, the vial containing biological cells frozen in ice is heated by the heater. (B) A schematic diagram showing the one-dimensional Stefan problem in a cylindrical coordinate system. The moving interface position is  $S$ . The solid temperature is  $\Theta_1$ . The liquid temperature is  $\Theta_2$ . The heater temperature is  $\Theta_b$ . All variables are written in dimensionless form.

where  $T$  is the temperature,  $r$  is the radial direction,  $t$  is time, and  $\alpha$  is the thermal diffusivity. Heat transfer associated with thawing at the moving solid-liquid interface is governed by the Stefan conditions

$$\rho \Delta H_f \frac{ds}{dt} = k_1 \frac{\partial T_1}{\partial r} - k_2 \frac{\partial T_2}{\partial r}, \quad (2)$$

$$T_1 = T_2 = T_m, \quad (3)$$

where  $s$  is the interface position,  $\Delta H_f$  is the latent heat of fusion,  $T_m$  is the melting point,  $\rho$  is the density,  $k$  is the thermal conductivity, and the subscripts 1 and 2 denote the solid and liquid phases, respectively. The above equations are nondimensionalized and discretized using the finite difference scheme with the method of lines, with appropriate boundary conditions, resulting in

$$\frac{d\Theta_1}{d\tau} = f_1(\Theta_1, \Theta_2, S), \quad (4)$$

$$\frac{d\Theta_2}{d\tau} = f_2(\Theta_1, \Theta_2, \Theta_b, S), \quad (5)$$

$$\frac{dS}{d\tau} = f_3(\Theta_1, \Theta_2, S), \quad (6)$$

$$(\Theta_1)_n = (\Theta_2)_0 = 0, \quad (7)$$

with the initial conditions

$$\Theta_1(\tau_0) = \Theta_2(\tau_0) = 0, \quad (8)$$

$$S(\tau_0) = 1, \quad (9)$$

where  $\Theta_1 \in \mathbb{R}^n$  collects the solid temperature  $(\Theta_1)_i$  for  $i = 0, \dots, n-1$ ;  $\Theta_2 \in \mathbb{R}^n$  collects the liquid temperature  $(\Theta_2)_j$  for  $j = 1, \dots, n$ ;  $S \in \mathbb{R}^1$  is the interface position;  $f_1 \in \mathbb{R}^n$ ,  $f_2 \in \mathbb{R}^n$ ,  $f_3 \in \mathbb{R}^1$  are the nonlinear functions;  $n$  is the number of grid points in each domain (set to 20);  $\tau \in [\tau_0, \tau_f]$  is the dimensionless time;  $\tau_0$  is the initial time; and  $\tau_f$  is the final time. Here (4) and (5) are derived from (1), while (6) and (7) correspond to (2) and (3), respectively. We refer to Srisuma et al. (2023b) for the detailed derivation of all equations, parameter values, and model validation.

In dimensionless form, the model consists of three main parts which describe the evolution of the solid temperature (4), the liquid temperature (5), and the interface po-

sition (6), respectively. The energy is continuously supplied to the system by the heater with the temperature  $\Theta_b$ . The system initially consists of pure solid, which corresponds to  $S = 1$ ; i.e., the interface position is at the outer boundary. As the thawing progresses, the interface position decreases and eventually becomes 0, indicating complete melting or pure liquid. The maximum temperature (dimensionless) is equal to 1, which is equivalent to  $37^\circ\text{C}$ , the maximum temperature recommended for cell thawing (Baboo et al., 2019; Uhrig et al., 2022). The minimum temperature (dimensionless) is equal to 0, corresponding to the melting point of  $-2^\circ\text{C}$ .

Finally, since the temperature varies spatially, we define the average temperature  $\Theta_{\text{avg}}$  as

$$\Theta_{\text{avg}} = \sum_{j=1}^n \frac{1}{n} (\Theta_2)_j. \quad (10)$$

In this case, only the liquid temperature  $\Theta_2$  is considered because the solid temperature  $\Theta_1$  is equal to the melting point, which does not change with time. Note that, as the problem is defined in the radial direction, the average temperature over the cross section could also be used instead of (10) for more accurate results. In any case, the implementation and algorithms presented later in this article are still valid for both definitions.

### 3 Optimal Control

#### 3.1 Optimal control formulation

The optimal control problem for cell thawing is

$$\begin{aligned} \min_{\Theta_b(\tau)} \mathcal{M}(\Theta_1(\tau_f), \Theta_2(\tau_f), S(\tau_f)) + \\ \int_{\tau_0}^{\tau_f} \mathcal{L}(\Theta_1(\tau), \Theta_2(\tau), S(\tau), \Theta_b(\tau), \tau) d\tau \end{aligned} \quad (11)$$

$$\begin{aligned} \text{s.t. Equations (4)–(9),} \\ 0 \leq \Theta_b(\tau) \leq 1. \end{aligned} \quad (12)$$

The control (aka decision variable, manipulated variable, input) of this optimal control problem is the heater temperature  $\Theta_b(\tau)$ . The mechanistic model (4)–(9) describes the physics of cell thawing, and thus serves as constraints. The lower and upper bounds of the heater temperature are represented by (12).

#### 3.2 Optimization-based approach

A detailed discussion on numerical algorithms to solve optimal control problems can be found in Nolasco et al. (2021). The common technique for solving optimal control problems is to discretize the partial differential equation (PDE) and ordinary differential equation (ODE) constraints, parameterize the time-varying control vector, and solve the resulting optimization problem numerically with a proper optimizer. This approach relies on the convergence of the optimization algorithm/solver to obtain the optimal control trajectory, and hence we denote this approach as the *optimization-based* approach.

In this article, six different optimization-based implementations that have been used widely in optimization and optimal control applications, including on a variety of software tools and programming languages, are considered:

- `opt_Ipopt`: The control vector is parameterized, and the resulting optimization is numerically solved by IPOPT (Wächter and Biegler, 2006), an open-source optimization solver for large-scale nonlinear optimization that has been implemented in various nonlinear and optimal control software packages. The IPOPT solver is employed in MATLAB via the OPTI Toolbox (Currie and Wilson, 2012). The system of ODEs is integrated by `ode15s`.
- `opt_fmincon`: The control vector is parameterized, and the resulting optimization is numerically solved by `fmincon`, a built-in optimization solver for constrained nonlinear optimization in MATLAB. The system of ODEs is integrated by `ode15s`.
- `opt_pfmincon`: The implementation is identical to `opt_fmincon` except that the parallel computing option for `fmincon` is turned on.
- `opt_sCasADi`: The optimal control problem is solved using CasADi (Andersson et al., 2019), a well-established open-source tool that has been widely used for nonlinear optimization, optimal control, and model predictive control. The problem is solved symbolically by the direct single shooting method via CasADi v3.6.3, with the code directly modified from the given example pack.
- `opt_mCasADi`: The implementation is similar to `opt_sCasADi` but uses the direct multiple shooting method instead.
- `opt_Gekko`: The optimal control problem is solved using GEKKO (Beal et al., 2018), a Python package for optimization and machine learning.

#### 3.3 Simulation-based approach

The approach in this article is inspired by a recent article on the optimal control of lithium-ion batteries (Berliner et al., 2022). The approach was motivated by the observation that the optimal control trajectories for that application moved from one active inequality constraint to another over time. That information was used to transform the optimal control problem into a mixed continuous-discrete system of index-1 DAEs in which existing software could be used to transition between active inequality constraints. This simulation-based technique eliminated the need for an optimization solver, resulting in a much more computationally efficient solution. No control vector parameterization is needed.

##### 3.3.1 Solution of high-index DAEs

In this work, we generalize the simulation-based technique for high-index DAE systems and apply the approach to solve multiple cell thawing problems. Various numerical algorithms for solving index-1 DAEs, including the implementation used in Berliner et al. (2022), fail when the differential index is higher than 1 (Petzold, 1982), and an increase in the differential index of DAEs leads to more difficulties in obtaining the numerical solution to DAEs (Campbell et al., 2008).

Many current DAE solvers are only capable of solving index-1 DAEs, so it is usually recommended to perform index reduction (e.g., `reduceDAEIndex` in MATLAB and `dae_index_lowering` in Julia) to transform a high-index system into an equivalent index-1 system, and then solve the resulting index-1 DAEs (Shampine et al., 1999; Campbell et al., 2008). This technique is usually suggested because index-1 DAEs can be solved easily by most DAE solvers, and so does not require specialized high-index DAE solvers. Nevertheless, there are two major drawbacks associated with index reduction. First, the index reduction process is costly when the number of states and differential index are huge. Second, index reduction could introduce a large number of new variables (sometimes called dummy derivatives (Mattsson and Söderlind, 1993)) to replace high-order derivatives, which unnecessarily increases the complexity of the problem. These issues are not commonly discussed in the literature as they become significant when the differential index is sufficiently large, e.g., Problem 3 in our case studies. Thus, this approach does not match our objective of accelerating the optimal control algorithm.

An alternative to the index reduction approach is to fully discretize a system of high-index DAEs (e.g., using a collocation method) and solve the discretized equations (Campbell et al., 2008). The specialized DAE solver in GEKKO employs the method of orthogonal collocation on finite elements to solve high-index DAEs (Beal et al., 2018). The main advantage of this implementation is that it does not have any constraint or limit on the differential index because index reduction and differentiation are not required (e.g., see detailed discussions by Hedengren et al. (2014) and Beal et al. (2018)). Hence, our DAE solutions for high-index systems rely on the DAE solver implemented in GEKKO.

### 3.3.2 Proposed algorithm

We denote this simulation-based approach as `sim_DAE`, which consists of three main steps. First, replace the objective function with algebraic equations, reformulating the original optimal control problem as a system of DAEs

$$g(\Theta_1(\tau), \Theta_2(\tau), S(\tau), \Theta_b(\tau), \tau) = 0. \quad (13)$$

The choice of algebraic equations is dependent on the objective function, which is demonstrated via the case studies presented in Section 4.

Second, treat the control variable ( $\Theta_b$  in this case) as a state instead of a decision variable. A consistent initial condition is required for this new state, and this initialization can be done in several ways, depending on the solver. For example, in GEKKO, the DAE solver does not strictly require a consistent initial condition, and so we can first guess some random initial condition and then run the DAE solver once to find the correct initial condition. Another possibility is to solve the optimization locally at the beginning of the process. Either approach requires minimal effort and computation, and so does not impact the overall computational performance. The initial condition for this new state is denoted by

$$\Theta_b(\tau_0) = \Theta_{b0}. \quad (14)$$

After obtaining the DAEs and initial conditions, the final step is to solve the resulting DAEs (13) and (14). As the control is now treated as a state, the optimal control vector can be obtained directly from the DAE solver.

This DAE reformulation technique inherently assumes that at least one of the constraints, bounds, or algebraic equations resulting from reformulating the objective function is active. For many practical problems in which this strong condition does not hold, the simulation-based approach is not guaranteed to produce an optimal solution, which is discussed in more detail in Section 4.3. Changes in the active constraints or bounds can be incorporated in the simulation using a simulation-switching technique, with Section 4.4 providing a discussion that includes references to several examples.

### 3.4 Implementation

Both optimization- and simulation-based techniques were implemented in MATLAB R2023a following the procedures introduced in Sections 3.2 and 3.3, with GEKKO called and executed in Python 3.10. The simulations were performed on a computer equipped with an Intel® Core™ i9-13950HX Processor CPU (24 cores) and 128 GB RAM on 64-bit Windows 11. The choice and justification of important solver options are given in Appendix B.

## 4 Case Studies

This section presents several optimal control problems for cell thawing to demonstrate the simulation-based technique and compare it with the optimization-based techniques. These examples are drawn from real problems and protocols associated with control and optimization of cell thawing and moving boundary problems. The case studies include both simple and complex problems to help illustrate the approach and assess the relationship between the comparative performance of the various algorithms and problem complexity.

### 4.1 Problem 1: Minimization of the thawing time

#### 4.1.1 Problem description and formulation

This first problem is simple and intuitive, with the solution known *a priori*, to demonstrate the simulation-based technique and validate all of our algorithms.

In general, it has been suggested that the heating process should be done rapidly to avoid potential damages to the cells and maintain high viability (Terry et al., 2010; Baboo et al., 2019; Hunt, 2019; Uhrig et al., 2022), which is equivalent to the optimal control problem

$$\begin{aligned} \min_{\Theta_b(\tau)} \quad & \tau_f \\ \text{s.t.} \quad & \text{Equations (4)–(9), (12)}. \end{aligned} \quad (15)$$

The solution to this optimal control problem is intuitive. To minimize the thawing time, the heater temperature should be fixed at its upper bound to provide the maximum heating power throughout the process.

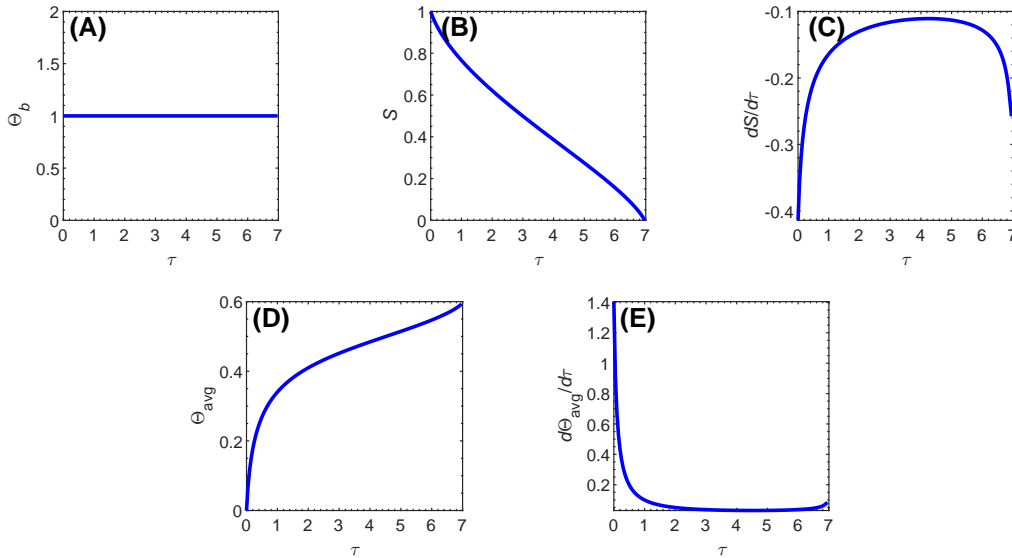


Fig. 2. Trajectories for the optimal (A) heater temperature  $\Theta_b$ , (B) interface position  $S$ , (C) interface velocity  $dS/d\tau$ , (D) average temperature  $\Theta_{\text{avg}}$ , and (E) rate of temperature change  $d\Theta_{\text{avg}}/d\tau$  in Problem 1.

#### 4.1.2 DAE Reformulation

To employ the simulation-based approach, (15) needs to be reformulated as a DAE system. In this problem, the control vector  $\Theta_b$  is treated as an algebraic state and explicitly specified an additional algebraic constraint  $\Theta_b(\tau) = 1$ . As a result, the equivalent system of DAEs for (15) is

$$\begin{aligned} \Theta_b(\tau) &= 1 \\ \text{Equations (4)–(9)}. \end{aligned} \quad (16)$$

The number of derivatives required to transform (16) into an equivalent ODE system is 1, hence an index-1 DAE system. This index-1 DAE system can be solved easily by most DAE solvers.

#### 4.1.3 Solution comparison

Every solution method gives the same optimal solution (Fig. 2); the heater temperature  $\Theta_b$  is at its upper bound of 1 all the time, ensuring that the algorithms and implementation are correct. The wall-clock time required for the simulation-based technique (sim\_DAE) is more than an order of magnitude lower than every optimization-based approach (Table 1). Optimization with GEKKO is the slowest method, followed by IPOPT, CasADi and `fmincon`. GEKKO's ODE solvers cannot perform adaptive time-stepping, which could lead to significantly slower computation. Parallel computing fails to accelerate `fmincon`. The simulation-based approach is the most computationally efficient algorithm in this case study.

### 4.2 Problem 2: Control of the average temperature

#### 4.2.1 Problem description and formulation

Besides using the fastest thawing as in Problem 1, some past studies considered cases in which the freezing and thawing rates are controlled, i.e., the rate of temperature change is kept constant (Seki and Mazur, 2008; Jang et al., 2017; Baboo et al., 2019; Bojic et al., 2021).

Table 1

Computational performance of each solution method for Problem 1.

Method	Wall time (s)
opt_Ipopt	$10.74 \pm 0.22$
opt_fmincon	$3.17 \pm 0.03$
opt_pfmincon	$3.23 \pm 0.06$
opt_sCasADi	$5.70 \pm 0.02$
opt_mCasADi	$5.81 \pm 0.06$
opt_Gekko	$34.08 \pm 0.31$
sim_DAE	$0.11 \pm 0.01$

As such, this problem focuses on controlling the rate of change in the average temperature during thawing by manipulating the heater temperature. The definition of the average temperature is as given in (10).

For a fixed heater temperature, the rate of temperature change is not constant (Figs. 2DE). Thus, the heater temperature needs to be manipulated. Consider the optimal control problem

$$\min_{\Theta_b(\tau)} \int_{\tau_0}^{\tau_F} \left( \frac{d\Theta_{\text{avg}}}{d\tau} - \left( \frac{d\Theta_{\text{avg}}}{d\tau} \right)_{\text{sp}} \right)^2 d\tau \quad (17)$$

$$\text{s.t. Equations (4)–(9), (12),}$$

where  $d\Theta_{\text{avg}}/d\tau$  is the rate of change in the average temperature and  $(d\Theta_{\text{avg}}/d\tau)_{\text{sp}}$  is the target value (setpoint) set to 0.04 for demonstration in this case study. For the optimization-based approaches, the control vector is parameterized using a piecewise linear function, with the number of control intervals  $n_c = 16$  (Appendix A).

#### 4.2.2 DAE Reformulation

For the simulation-based technique, first analyze the objective function in (17). This objective function is minimized when the rate of change in average temperature is equal to the setpoint. Replacing the objective func-

tion in (17) with the algebraic equation  $d\Theta_{\text{avg}}/d\tau = (d\Theta_{\text{avg}}/d\tau)_{\text{sp}}$  results in the system of DAEs

$$\frac{d}{d\tau} \left( \sum_{j=1}^n \frac{1}{n} (\Theta_2)_j \right) = \left( \frac{d\Theta_{\text{avg}}}{d\tau} \right)_{\text{sp}}, \quad (18)$$

Equations (4)–(9), (14),

where  $\Theta_b$  is now treated as a state. The differential index of (18) is 2, which can be solved using GEKKO as explained in Section 3.3.

#### 4.2.3 Solution comparison

To evaluate the correctness of the solution, define the error measured by a modified 2-norm for this problem as

$$\|e\|_2 = \sqrt{\frac{1}{n_k} \sum_{k=1}^{n_k} \left( \left( \frac{d\Theta_{\text{avg}}}{d\tau} \right)_k - \left( \frac{d\Theta_{\text{avg}}}{d\tau} \right)_{\text{sp}} \right)^2}, \quad (19)$$

where  $(d\Theta_{\text{avg}}/d\tau)_k$  is the rate of change in average temperature resulting from solving (17) or (18) evaluated at each time point  $k$  in the time span  $[\tau_0, \tau_f]$  and  $n_k$  is the number of sampling time points. Small  $\|e\|_2$  corresponds to the rate of change in average temperature being close to the target value, indicating that the heater temperature is optimal; i.e., the solution method is accurate.

The optimal solutions to Problem 2 obtained from the optimization- and simulation-based approaches are illustrated in Fig. 3. Most solution techniques predict the same heater temperature profile except the methods with `fmincon` that predict a slightly higher temperature (Fig. 3A). As time progresses, the heater temperature increases to compensate for a reduction in the temperature difference (driving force) between the heater and product. The rate of change in average temperature can be controlled nearly perfectly at 0.04 for IPOPT, CasADi, GEKKO, and the simulation-based method, while this value fluctuates up to about 0.046 for `fmincon`, implying that `fmincon` fails to converge to the optimal solution in this case (Fig. 3B). It is also evident that the average temperature increases linearly at the rate of 0.04 in all cases except for `fmincon` (Fig. 3C).

Table 2  
Computational performance and accuracy of each solution method for Problem 2.

Method	Wall time (s)	$\ e\ _2$
opt_Ipopt	162.67 ± 3.72	8.03 × 10 <sup>-5</sup>
opt_fmincon	349.07 ± 11.67	1.21 × 10 <sup>-3</sup>
opt_pfmincon	79.40 ± 1.57	1.21 × 10 <sup>-3</sup>
opt_sCasADi	363.36 ± 12.52	8.04 × 10 <sup>-5</sup>
opt_mCasADi	5189.15 ± 71.42	8.04 × 10 <sup>-5</sup>
opt_Gekko	191.89 ± 4.86	4.91 × 10 <sup>-5</sup>
sim_DAE	3.71 ± 0.15	2.25 × 10 <sup>-5</sup>

The simulation-based approach is by far the fastest solution method, accelerating the computation by 40× to 90× compared to the typical solvers IPOPT and `fmincon` (Table 2). Without parallel computing, optimization with IPOPT is fastest, followed by GEKKO,

`fmincon`, and CasADi. Parallel computing can significantly reduce the computation time for `fmincon`. With the direct multiple shooting method (`opt_mCasADi`), the number of states resulting from spatial discretization is large. For example, with  $n = 20$ , there are 41 states for each control interval and 656 states for  $n_c = 16$ . This large nonlinear optimization is computationally expensive to solve compared to other approaches. In terms of accuracy, `fmincon` produces the largest error, which is about 30–40 fold higher than for the other techniques. This indicates that the solution obtained from `fmincon` is not optimal, agreeing with the plots shown in Fig. 3. Although both `fmincon` and IPOPT employ the interior point methods, the detailed implementations (e.g., gradient/hessian calculation, scaling) are not exactly the same, which could result in different accuracy and performance (see detailed discussion and comparison of these solvers in Rojas-Labanda and Stolpe (2015)). The simulation-based and other optimization-based methods except `fmincon` have similar accuracy. Despite an increase in the differential index, the simulation-based approach is still much faster than the optimization-based techniques while giving the same level of accuracy.

### 4.3 Problem 3: Control of the interface velocity

#### 4.3.1 Problem description and formulation

One of the primary interests in a Stefan problem is the moving solid-liquid interface. The literature has studied and shown the importance of interface position tracking and optimization in various applications (Hill and Wu, 1994; Brezina et al., 2018; Srisuma et al., 2023b, for example). This problem focuses on the control of the interface velocity, i.e., the evolution of a melting/freezing process.

Consider the optimal control problem

$$\min_{\Theta_b(\tau)} \int_{\tau_0}^{\tau_f} \left( \frac{dS}{d\tau} - \left( \frac{dS}{d\tau} \right)_{\text{sp}} \right)^2 d\tau \quad (20)$$

s.t. Equations (4)–(9), (12),

where  $dS/d\tau$  is the interface velocity and  $(dS/d\tau)_{\text{sp}}$  is the target velocity set to  $-0.1$  for demonstration in this case study. In Problem 1 (Fig. 2BC), the velocity of the moving interface is not constant if the heater temperature is fixed. In this case study, the aim is to control the velocity of the moving interface to be constant at  $(dS/d\tau)_{\text{sp}}$  by manipulating the heater temperature throughout the process as formulated in (20). For the optimization-based approaches, the control vector is parameterized using a piecewise linear function, with the number of control intervals  $n_c = 12$  (see Appendix A).

#### 4.3.2 DAE Reformulation

To apply the simulation-based technique, a similar approach used in Problem 2 can be used, but here we instead enforce the moving interface velocity by modifying the interface equation (6) to be equal to  $(dS/d\tau)_{\text{sp}}$ .

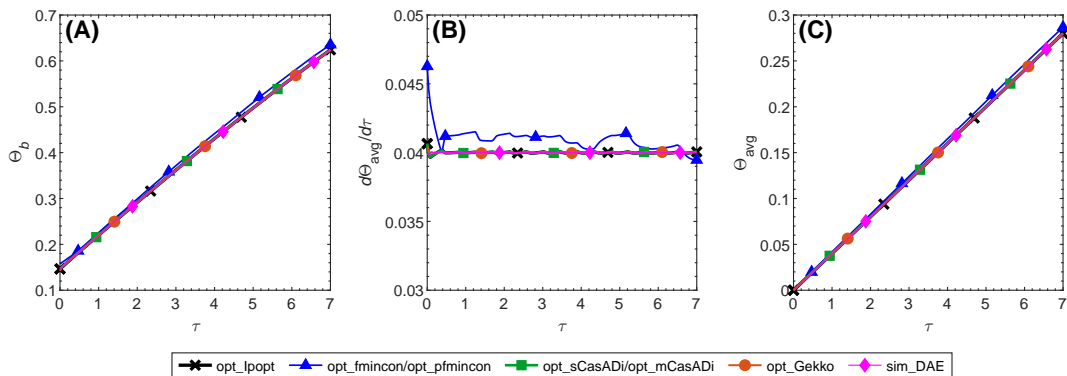


Fig. 3. Trajectories for the optimal (A) heater temperature, (B) rate of change in average temperature, and (C) average temperature simulated via the optimization- and simulation-based approaches in Problem 2.

Consequently, (20) is reformulated as the DAE system

$$\frac{dS}{d\tau} = f_3(\Theta_1, \Theta_2, S) = \left( \frac{dS}{d\tau} \right)_{sp}, \quad (21)$$

Equations (4), (5), (7)–(9), (14).

The differential index of (21) is  $n$ , which is the number of grid points resulting from spatial discretization. Therefore, if the spatial discretization of the domain is made finer to increase numerical accuracy, the differential index of (21) increases. In this case,  $n = 20$ , and hence (21) becomes an index-20 DAE system, making the problem even more complicated and difficult to solve compared to the index-2 system in Problem 2.

To explore the possibility of using the index reduction technique, MATLAB’s `reduceDAEIndex` was used to reduce the differential index of (21). However, the index reduction process was not complete even after 20 hours of simulation. Obviously, this technique is not feasible for our problem as mentioned before in Section 3.3. Therefore, GEKKO’s DAE solver is needed.

#### 4.3.3 Solution comparison

Similar to Problem 2, we define the error measured by a modified 2-norm for this problem as

$$\|e\|_2 = \sqrt{\frac{1}{n_k} \sum_{k=1}^{n_k} \left( \left( \frac{dS}{d\tau} \right)_k - \left( \frac{dS}{d\tau} \right)_{sp} \right)^2}, \quad (22)$$

where  $(dS/d\tau)_k$  is the interface velocity resulting from solving (20) or (21) evaluated at each time point  $k$  in the time span  $[\tau_0, \tau_f]$ .

The optimal solutions to Problem 3 are shown in Fig. 4. The optimal heater temperature predicted by each technique is nearly identical except that there is a large drop around the end of the process for the `fmincon` cases (Fig. 4A). The interface velocity can be controlled at about  $-0.1$  all the time for IPOPT, CasADi, GEKKO, and the simulation-based technique, while some fluctuation is observed for `fmincon` (Fig. 4B). This indicates that `fmincon` is less accurate than the others approaches, which is a similar trend observed before in Problem 2. With the interface velocity controlled, the interface position recedes linearly at the rate of 0.1 (Fig. 4C).

For the computational performance, the simulation-based technique is about  $60\times$  to  $900\times$  faster than all of the optimization-based approaches (Table 3). IPOPT, GEKKO, and CasADi are comparable for the direct single shooting method, while the multiple shooting method is much slower. Parallel computing can significantly accelerate `fmincon` but is still much slower than the simulation-based approach. `fmincon` is the least accurate method; the error is higher than for the other approaches by more than an order of magnitude. Except for `fmincon`, the simulation-based approach has similar accuracy as the optimization-based approaches, with the error of about  $2\times 10^{-5}$ .

Table 3

Computational performance and accuracy of each solution method for Problem 3.

Method	Wall time (s)	$\ e\ _2$
opt_Ipopt	214.01 ± 5.75	$1.96\times 10^{-5}$
opt_fmincon	317.89 ± 5.46	$3.05\times 10^{-4}$
opt_pfmincon	92.30 ± 1.52	$3.05\times 10^{-4}$
opt_sCasADi	225.42 ± 5.92	$1.96\times 10^{-5}$
opt_mCasADi	2618.13 ± 83.29	$1.97\times 10^{-5}$
opt_Gekko	179.77 ± 2.45	$4.37\times 10^{-5}$
sim_DAE	2.99 ± 0.07	$2.41\times 10^{-5}$

From the three case studies, the simulation-based approach reliably solves the optimal control problems irrespective of the differential index, ranging from a simple index-1 problem to an extremely high-index DAE system. The approach is much faster than any optimization-based technique while giving the same level of accuracy.

The simulation-based approach, however, has one limitation associated with the DAE reformulation. As described in Section 3.3, the DAE reformulation is guaranteed to be optimal when at least one of the constraints, bounds, or algebraic equations resulting from reformulating the objective function is active. This is typically the case when the objective function of the original optimal control problem can be minimized by solving each subproblem resulting from control vector parameterization individually – in other words, local minimization at every control/time interval (subproblem) is equivalent to global minimization of the whole process (original problem). For example, in Problem 1, if the thawing time of every control interval is minimized, the total thawing time is automatically minimized. In Problems 2 and 3, if the rate of temperature change and interface velocity

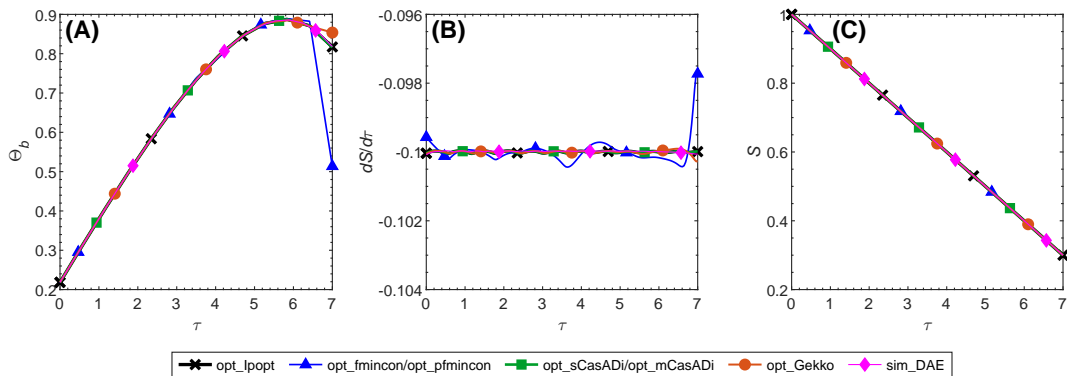


Fig. 4. Trajectories for the optimal (A) heater temperature, (B) interface velocity, and (C) interface position via the optimization- and simulation-based approaches in Problem 3.

are controlled locally for each control interval, the whole process is also controlled. These objective functions are common in many applications, for which the simulation-based technique can be applied, including lithium-ion batteries of various chemistries (Berliner et al., 2022; Galuppini et al., 2023; Matschek et al., 2023) and microwave lyophilization (Srisuma et al., 2023a). An example of a system in which the method is not optimal is a reactor with multiple chemical reactions, with the goal of maximizing the amount of desired product at the end of the process. Maximizing the amount of product during the first control interval could concurrently increase the amount of some byproducts that can degrade the desired product later. In this situation, local optimization is not equivalent to global optimization. As such, an algebraic equation/constraint may not be active, so an optimization-based technique is needed. Although the simulation-based approach does not give an optimal solution to such problems, it can be used to provide an initialization to the optimization solver.

#### 4.4 Problem 4: Sensitivity analysis

In Problems 2 and 3, the simulation-based approach is tested with one value of  $(d\Theta_{\text{avg}}/d\tau)_{\text{sp}}$  and  $(dS/d\tau)_{\text{sp}}$ , which are 0.04 and  $-0.1$ , respectively. To demonstrate the robustness of our framework, this section conducts a sensitivity analysis by varying  $(d\Theta_{\text{avg}}/d\tau)_{\text{sp}}$  and  $(dS/d\tau)_{\text{sp}}$  and employs the simulation-based approach to solve the problems.

The simulation-based approach provides accurate solutions irrespective of the values of  $(d\Theta_{\text{avg}}/d\tau)_{\text{sp}}$  and  $(dS/d\tau)_{\text{sp}}$  (Figs. 5 and 6). The rate of change in average temperature and interface velocity are at the setpoints except for  $(dS/d\tau)_{\text{sp}} = -0.15$ . An interface velocity of  $-0.15$  is too fast for the given heater temperature, so the upper bound is active, and that the heater temperature cannot be increased further to achieve the target velocity. The target velocity that is larger (smaller in magnitude) than the peak of Fig. 2C, which about  $-0.12$ , will never violate the bound (see Appendix C for a formal proof).

For cases where the bound is active, a simulation switching technique can be used to transition between active constraints, resulting in a hybrid discrete/continuous dynamic simulation (Feehery and Barton, 1998; Barton et al., 2000; Berliner et al., 2022). First, initialize a DAE

simulation as usual. Next, terminate the current simulation when the bound on any control vector is active and then initialize a new DAE simulation with that active bound/constraint. Perform this switching whenever there is a change in the active constraints, which results in a mixed continuous-discrete DAE system instead of a pure continuous system. The complexity of this procedure depends on the choice of a DAE solver. For example, MATLAB’s and Julia’s DAE solvers have a built-in function to track all variables and terminate a simulation when the specified condition (aka event) is met, which facilitates the implementation of such switching. The switching technique can also be used to handle cases where the control trajectory is discontinuous (see examples in Berliner et al. (2022); Srisuma et al. (2023a)). GEKKO’s DAE solvers, on the other hand, do not have a built-in option for handling switches, and so this process needs to be executed manually (see our software/code for implementation). This switching technique can also be used for path constraints.

With this capability, the benefit of the simulation-based approach is even more substantial in applications where a large number of simulation runs are required, e.g., parametric studies and design optimization.

## 5 Conclusion

This article describes a new approach for determining control and state trajectories in optimal control problems by reformulation as a system of DAEs. The optimal control and state vectors are obtained via simulation of the resulting DAE system with the selected DAE solver, eliminating the need for an optimization solver and thus greatly accelerating the computation.

Our proposed framework was demonstrated and benchmarked against a variety of optimization-based approaches – IPOPT, fmincon, CasADi, and GEKKO – for case studies involving the optimal control of a Stefan problem for cell thawing. The case studies include the minimization of the thawing time, the control of the average temperature, and the control of the interface velocity, transformed into DAE systems of index 1, 2, and 20, respectively. At the same level of accuracy, the simulation-based approach is more than an order of magnitude faster than every optimization-based method in all cases. The simulation-based approach offers an



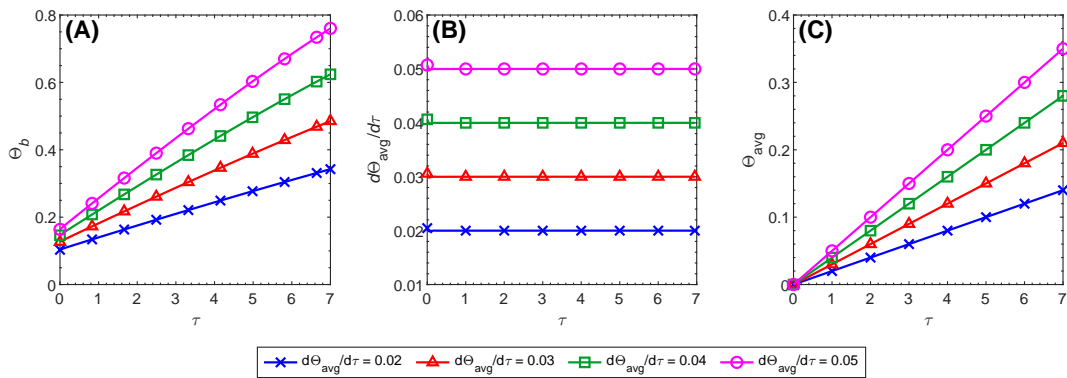


Fig. 5. Trajectories for the optimal (A) heater temperature, (B) rate of change in average temperature, and (C) average temperature simulated via the simulation-based approach at four different values of  $(d\Theta_{\text{avg}}/d\tau)_{\text{sp}}$  in Problem 4.

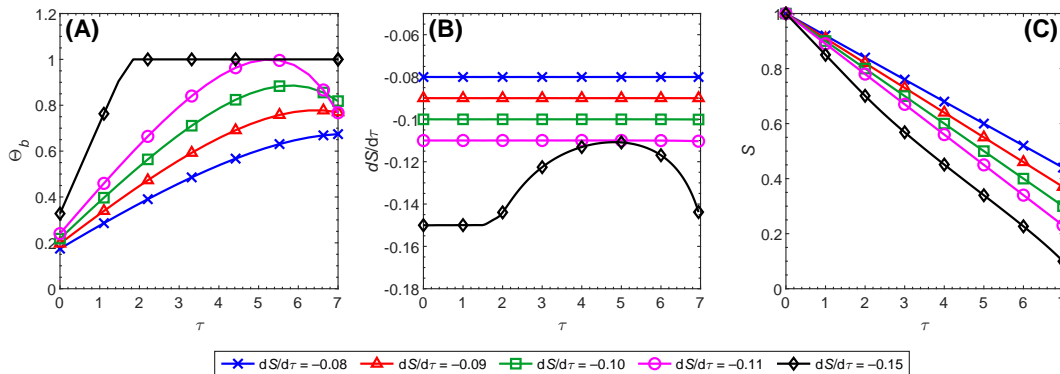


Fig. 6. Trajectories for the optimal (A) heater temperature, (B) interface velocity, and (C) interface position simulated via the simulation-based approach at four different values of  $(dS/d\tau)_{\text{sp}}$  in Problem 4.

efficient and reliable framework for solving the optimal control problems, serving as a promising alternative to the traditional techniques in applications where speed is crucial, e.g., real-time online model predictive control.

Some future directions of interest are to (1) generalize the approach and (2) improve the computational performance. The ultimate goal is a highly efficient optimal control solver applicable to problems with a variety of objective functions and constraints that arise in multiple fields. Implementation would be simplified if high-index DAE solvers become available that have built-in options for mixed continuous-discrete simulation.

## Data Availability

All software and data will be made available upon publication of the manuscript.

## Acknowledgments

The authors would like to thank Dr. John D. Hedengren for advice on the software GEKKO.

## Appendices

### A Control Vector Parameterization

#### A.1 Piecewise constant and linear controls

Piecewise constant and linear controls are most common in optimal control (Nolasco et al., 2021). This section

justifies the use of piecewise linear controls in Problems 2 and 3 for the optimization-based approaches, in comparison to piecewise constant controls. This comparison considers the most complex problem (Problem 3), with `opt_Ipopt` as the solver.

Table A.1

Comparison between the errors  $\|e\|_2$  resulting from piecewise constant and linear control vector parameterization for different values of control intervals  $n_c$ .

$n_c$	Error measured by $\ e\ _2$	
	Piecewise constant	Piecewise linear
4	0.012	$3.01 \times 10^{-4}$
8	0.010	$5.68 \times 10^{-5}$
12	0.012	$1.96 \times 10^{-5}$

From Table A.1, the piecewise linear control is more accurate than the piecewise constant control by many orders of magnitude. Since the dynamics of the interface position and average temperature are highly nonlinear, a large value of  $n_c$  is required for a piecewise constant control to accurately manipulate the average temperature and moving interface, leading to a much larger nonlinear program that is computationally expensive and difficult to converge. As a result, a piecewise linear control is selected in this work.

#### A.2 Number of control intervals

The accuracy of the optimization-based solution is influenced by the number of control intervals  $n_c$ . This section justifies those numbers by investigating the effect of  $n_c$  on the accuracy of the solution.

The optimal control problems defined by (17) and (20) were solved via `opt_Ipopt` and  $\|e\|_2$  was calculated for different values of  $n_c$ . Logically, the accuracy of the solution should improve, i.e., smaller  $\|e\|_2$ , when  $n_c$  increases due to finer discretization. From Fig. A.1, the accuracy of the solution does not change significantly after  $n_c$  reaches some certain value, and so this threshold should be chosen for control vector parameterization. As a result,  $n_c$  was set to 16 for Problem 2 (Fig. A.1A) and 12 for Problem 3 (Fig. A.1B).

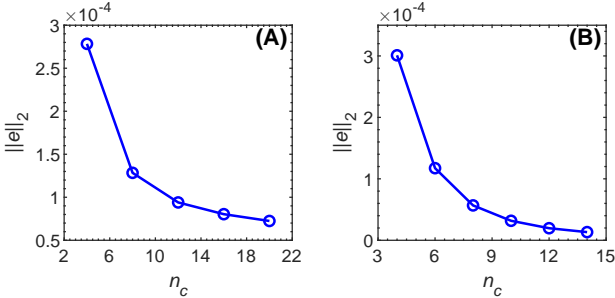


Fig. A.1. Errors measured by  $\|e\|_2$  for different values of control intervals  $n_c$  for (A) Problem 2 and (B) Problem 3.

## B Solver Options

There are a large number of options for optimization, ODE, and DAE solvers, which could lead to different accuracy and computational performance. This section describes and justifies the choice of important solver options used in this work. The default values were used for the options not mentioned here.

For all case studies, index-1 DAEs were solved by `ode15s` in MATLAB, whereas high-index DAEs were handled by GEKKO in Python. The differential index of DAEs was checked using `reduceDAEIndex`. The wall-clock times (aka wall times, clock times) were measured using the `tic` and `toc` functions, with each simulation repeated at least 10 times for consistent results, as indicated by the standard deviation of the measured wall times being smaller than 5%. For fair comparison of computational performance, the initial guess of  $\Theta_b$  was set to the average value of 0.5 in all cases.

For the optimization-based approaches, the optimality tolerance was set to  $10^{-7}$  for all optimization solvers, including IPOPT, `fmincon`, CasADi, and GEKKO. The integration tolerance for `ode15s` was set to  $10^{-10}$ . Using higher values for the optimality and integration tolerances could lead to inaccurate solutions, while using tighter values does not improve the accuracy significantly. For the objective functions (17) and (20) in Problems 2 and 3, the derivatives were approximated using a finite difference scheme, whereas the integrals can be approximated using a Riemann sum. The time step  $\Delta\tau$  was set to 0.05.

While `ode15s` uses adaptive time-stepping, this option is not available in GEKKO; i.e., users have to specify a vector of time points for ODE integration. Hence, there is no ideal comparison between GEKKO’s ODE solvers and MATLAB’s `ode15s`. The fixed time step  $\Delta\tau = 0.05$  was specified for ODE integration in GEKKO, with five collocation points (`INODES = 5`) for each time interval. This time step was chosen to be consistent with the

value used for a finite difference and Riemann sum approximation mentioned in the previous paragraph, while the number of collocation points was selected such that the temperature and interface position simulated by GEKKO’s ODE solver have the same level of accuracy as those simulated by `ode15s`.

For the simulation-based approach, `ode15s` was used for an index-1 system (Problem 1), with the exact same solver options as mentioned above. GEKKO’s DAE solver was used for high-index systems (Problems 2 and 3). As a reformulated DAE system is different from the original ODE system, the time step needs to be adjusted accordingly. The time step was selected such that the accuracy of the simulation-based solution measured by  $\|e\|_2$  is on the same order of magnitude as that of the optimization-based solution, giving  $\Delta\tau = 0.12$  and  $\Delta\tau = 0.37$  for Problems 2 and 3, respectively.

The accuracy of both the optimization- and simulation-based approaches is measured using  $\|e\|_2$  defined by (19) and (22). To calculate  $\|e\|_2$ , the derivatives were approximated using a finite difference scheme with  $\Delta\tau = 0.05$ .

## C Bounds on the Interface Velocity and Rate of Change in Temperature

We show in Fig. 2, Problems 2 and 3, and Section 4.4 that, if the target velocity (and also the rate of temperature change) is chosen properly, the bound on a control vector will never be violated. A formal proof is given in this section.

To obtain a closed-form solution for the proof, the heat conduction in the liquid domain is assumed to be quasi-steady. This approximation is accurate for problems associated with phase change as most of the heat transfer occurs at the moving interface. In this case, the closed-form solution for the interface velocity is

$$\frac{dS}{d\tau} = -\frac{k_2 U \Theta_b (T_0 - T_m)}{\rho L \alpha_1 S (U \ln(1/S) + k/b)}, \quad (\text{C.1})$$

where all the parameter description and values can be found in [Srisuma et al. \(2023b\)](#). From (C.1), the interface velocity ( $dS/d\tau$ ) is a monotonic function of the heater temperature ( $\Theta_b$ ). Hence, the condition in which the bounds on the heater temperature are not violated can be obtained by substituting the upper bound  $\Theta_b = 1$  into (C.1), which is

$$\left(\frac{dS}{d\tau}\right)_{\text{sp}} > -\frac{k_2 U (T_0 - T_m)}{\rho \alpha_1 \Delta H_f S (U \ln(1/S) + k/b)}. \quad (\text{C.2})$$

With the parameter values in [Srisuma et al. \(2023b\)](#), the right-hand side of (C.2) is about  $-0.13$ . This conclusion agrees with the results presented in Problems 3 and 4, in which the bounds are not violated when  $(dS/d\tau)_{\text{sp}}$  is higher than  $-0.13$ , whereas the upper bound is active when  $(dS/d\tau)_{\text{sp}}$  is  $-0.15$ . A similar strategy can be used for analyzing the temperature change, e.g., using a thermal lumped capacity approximation.

Note that our simulation-based approach does not require to know *a priori* if the bounds will be active or not, as the upper and lower bounds can be handled as shown in Problem 4.

## References

- Andersson, J.A.E., Gillis, J., Horn, G., Rawlings, J.B., Diehl, M., 2019. CasADi: A software framework for nonlinear optimization and optimal control. *Mathematical Programming Computation* 11, 1–36.
- Baboo, J., Kilbride, P., Delahaye, M., Milne, S., Fonseca, F., Blanco, M., Meneghel, J., Nancekievill, A., Gaddum, N., Morris, G.J., 2019. The impact of varying cooling and thawing rates on the quality of cryopreserved human peripheral blood T cells. *Scientific Reports* 9, 3417.
- Barton, P., Banga, J., Galán, S., 2000. Optimization of hybrid discrete/continuous dynamic systems. *Computers & Chemical Engineering* 24, 2171–2182.
- Beal, L., Hill, D., Martin, R., Hedengren, J., 2018. GEKKO optimization suite. *Processes* 6, 106.
- Berliner, M.D., Jiang, B., Cogswell, D.A., Bazant, M.Z., Braatz, R.D., 2022. Novel operating modes for the charging of lithium-ion batteries. *Journal of The Electrochemical Society* 169, 100546.
- Biegler, L.T., 2007. An overview of simultaneous strategies for dynamic optimization. *Chemical Engineering and Processing: Process Intensification* 46, 1043–1053.
- Bird, R.B., Stewart, W.E., Lightfoot, E.N., 2002. *Transport Phenomena*. Second ed., John Wiley & Sons, New York.
- Bojic, S., Murray, A., Bentley, B.L., Spindler, R., Pawlik, P., Cordeiro, J.L., Bauer, R., de Magalhães, J.P., 2021. Winter is coming: the future of cryopreservation. *BMC Biology* 19, 56.
- Brezina, M., Klimes, L., Stetina, J., 2018. Optimization of material properties of phase change materials for latent heat thermal energy storage. *MENDEL* 24, 47–54.
- Brosa Planella, F., Please, C.P., Van Gorder, R.A., 2019. Extended Stefan problem for solidification of binary alloys in a finite planar domain. *SIAM Journal on Applied Mathematics* 79, 876–913.
- Brosa Planella, F., Please, C.P., Van Gorder, R.A., 2021. Extended Stefan problem for the solidification of binary alloys in a sphere. *European Journal of Applied Mathematics* 32, 242–279.
- Campbell, S.L., Linh, V.H., Petzold, L.R., 2008. Differential-algebraic equations. *Scholarpedia* 3, 2849.
- Carslaw, H., Jaeger, J., 1959. *Conduction of Heat in Solids*. Second ed., Oxford University Press, London.
- Chen, Z., Bentsman, J., Thomas, B.G., 2019. Optimal control of free boundary of a Stefan problem for metallurgical length maintenance in continuous steel casting, in: *American Control Conference*, pp. 3206–3211.
- Cottle, C., Porter, A.P., Lipat, A., Turner-Lyles, C., Nguyen, J., Moll, G., Chinnadurai, R., 2022. Impact of cryopreservation and freeze-thawing on therapeutic properties of mesenchymal stromal/stem cells and other common cellular therapeutics. *Current Stem Cell Reports* 8, 72–92.
- Currie, J., Wilson, D.I., 2012. OPTI: Lowering the barrier between open source optimizers and the industrial MATLAB user, in: Sahinidis, N., Pinto, J. (Eds.), *Foundations of Computer-Aided Process Operations*. Dalwadi, M.P., Waters, S.L., Byrne, H.M., Hewitt, I.J., 2020. A mathematical framework for developing freezing protocols in the cryopreservation of cells. *SIAM Journal on Applied Mathematics* 80, 657–689.
- Feehery, W.F., Barton, P.I., 1998. Dynamic optimization with state variable path constraints. This research was supported by the United States Department of Energy under grant de-fg02-94er14447. *Computers & Chemical Engineering* 22, 1241–1256.
- Galuppini, G., Berliner, M.D., Lian, H., Zhuang, D., Bazant, M.Z., Braatz, R.D., 2023. Efficient computation of safe, fast charging protocols for multiphase lithium-ion batteries: A lithium iron phosphate case study. *Journal of Power Sources* 580, 233272.
- Gusev, A.O., Shcheritsa, O.V., Mazhorova, O.S., 2021. Two equivalent finite volume schemes for Stefan problem on boundary-fitted grids: Front-tracking and front-fixing techniques. *Differential Equations* 57, 876–890.
- Hedengren, J.D., Shishavan, R.A., Powell, K.M., Edgar, T.F., 2014. Nonlinear modeling, estimation and predictive control in APMonitor. *Computers & Chemical Engineering* 70, 133–148.
- Hill, J.M., Wu, Y.H., 1994. On a nonlinear Stefan problem arising in the continuous casting of steel. *Acta Mechanica* 107, 183–198.
- Hinze, M., Ziegenbalg, S., 2007. Optimal control of the free boundary in a two-phase Stefan problem. *Journal of Computational Physics* 223, 657–684.
- Hunt, C.J., 2019. Technical considerations in the freezing, low-temperature storage and thawing of stem cells for cellular therapies. *Transfusion Medicine and Hemotherapy* 46, 134–149.
- Jang, T.H., Park, S.C., Yang, J.H., Kim, J.Y., Seok, J.H., Park, U.S., Choi, C.W., Lee, S.R., Han, J., 2017. Cryopreservation and its clinical applications. *Integrative Medicine Research* 6, 12–18.
- Kishida, M., Ford Versypt, A.N., Pack, D.W., Braatz, R.D., 2013. Optimal control of one-dimensional cellular uptake in tissue engineering. *Optimal Control Applications and Methods* 34, 680–695.
- Kurbatova, G.I., Ermolaeva, N.N., 2019. An effective algorithm of the numerical solution to the Stefan problem. *Journal of Physics: Conference Series* 1392, 012034.
- Matschek, J., Berliner, M.D., Himmel, A., Braatz, R.D., Findeisen, R., 2023. Necessary optimality conditions for fast lithium-ion battery charging via hybrid simulations, in: *American Control Conference*, pp. 3783–3789.
- Mattsson, S.E., Söderlind, G., 1993. Index reduction in differential-algebraic equations using dummy derivatives. *SIAM Journal on Scientific Computing* 14, 677–692.
- Mellefont, D., Sargent, R., 1978. Calculation of optimal controls of specified accuracy. *Journal of Optimization Theory and Applications* 25, 407–414.
- Mesbah, A., Ford Versypt, A.N., Zhu, X., Braatz, R.D., 2014. Nonlinear model-based control of thin-film drying for continuous pharmaceutical manufacturing. *Industrial & Engineering Chemistry Research* 53, 7447–7460.
- Meyer, G.H., 1971. A numerical method for two-phase

- Stefan problems. *SIAM Journal on Numerical Analysis* 8, 555–568.
- Mikova, V.V., Kurbatova, G.I., Ermolaeva, N.N., 2017. Analytical and numerical solutions to Stefan problem in model of the glaciation dynamics of the multilayer cylinder in sea water. *Journal of Physics: Conference Series* 929, 012103.
- Miyaoka, T., Kawahara, M., 2008. Optimal control of drainage basin considering moving boundary. *International Journal of Computational Fluid Dynamics* 22, 677–686.
- Neuman, C., Sen, A., 1974. Weighted residual methods in optimal control. *IEEE Transactions on Automatic Control* 19, 67–69.
- Nolasco, E., Vassiliadis, V.S., Kähm, W., Adloor, S.D., Ismaili, R.A., Conejeros, R., Espaa, T., Gangadharan, N., Mappas, V., Scott, F., Zhang, Q., 2021. Optimal control in chemical engineering: Past, present and future. *Computers & Chemical Engineering* 155, 107528.
- Pawlow, I., 1987. Optimal control of two-phase Stefan problems - numerical solutions, in: Hoffmann, K.H., Krabs, W. (Eds.), *Optimal Control of Partial Differential Equations II: Theory and Applications*. Birkhäuser Basel, Basel, pp. 179–206.
- Petrus, B., Bentsman, J., Thomas, B.G., 2010. Feedback control of the two-phase Stefan problem, with an application to the continuous casting of steel, in: 49th IEEE Conference on Decision and Control, pp. 1731–1736.
- Petzold, L., 1982. Differential/algebraic equations are not ODE's. *SIAM Journal on Scientific and Statistical Computing* 3, 367–384.
- Rabin, Y., Shitzer, A., 1995. Exact solution to the one-dimensional inverse-Stefan problem in nonideal biological tissues. *Journal of Heat Transfer* 117, 425–431.
- Rabin, Y., Shitzer, A., 1997. Combined solution of the inverse Stefan problem for successive freezing/thawing in nonideal biological tissues. *Journal of Biomechanical Engineering* 119, 146–152.
- Rodrigues, H.S., Monteiro, M.T.T., Torres, D.F.M., 2014. Optimal control and numerical software: An overview, in: Miranda, F. (Ed.), *Systems Theory: Perspectives, Applications and Developments*. Nova Science Publishers, New York, pp. 93–110.
- Rojas-Labanda, S., Stolpe, M., 2015. Benchmarking optimization solvers for structural topology optimization. *Structural and Multidisciplinary Optimization* 52, 527–547.
- Roubíček, T., 1986. Optimal control of a Stefan problem with state-space constraints. *Numerische Mathematik* 50, 723–744.
- Sargent, R.W.H., Sullivan, G.R., 1978. The development of an efficient optimal control package, in: Stoer, J. (Ed.), *Optimization Techniques: Proceedings of the 8th IFIP Conference on Optimization Techniques*, pp. 158–168.
- Scott, F., Wilson, P., Conejeros, R., Vassiliadis, V.S., 2018. Simulation and optimization of dynamic flux balance analysis models using an interior point method reformulation. *Computers & Chemical Engineering* 119, 152–170.
- Seki, S., Mazur, P., 2008. Effect of warming rate on the survival of vitrified mouse oocytes and on the recrystallization of intracellular ice. *Biology of Reproduction* 79, 727–737.
- Shampine, L.F., Reichelt, M.W., Kierzenka, J.A., 1999. Solving index-1 DAEs in MATLAB and Simulink. *SIAM Review* 41, 538–552.
- Silva Neto, A.J., White, R.E., 1994. Numerical control of the Stefan problem: Maximum melting. *Computer Methods in Applied Mechanics and Engineering* 113, 351–362.
- Srisuma, P., Barbastathis, G., Braatz, R.D., 2023a. Analytical solutions for the modeling, optimization, and control of microwave-assisted freeze drying. *Computers & Chemical Engineering* 177, 108318.
- Srisuma, P., Barbastathis, G., Braatz, R.D., 2024. Simulation-based approach for optimal control of a stefan problem, in: *American Control Conference*, pp. 3031–3036.
- Srisuma, P., Pandit, A., Zhang, Q., Hong, M.S., Gamekkanda, J., Fachin, F., Moore, N., Djordjevic, D., Schwaerzler, M., Oyetunde, T., Tang, W., Myerson, A.S., Barbastathis, G., Braatz, R.D., 2023b. Thermal imaging-based state estimation of a Stefan problem with application to cell thawing. *Computers & Chemical Engineering* 173, 108179.
- Tao, L.N., 1979. The Stefan problem of a polymorphous material. *Journal of Applied Mechanics* 46, 789–794.
- Terry, C., Dhawan, A., Ragai R. Mitry, S.C.L., Hughes, R.D., 2010. Optimization of the cryopreservation and thawing protocol for human hepatocytes for use in cell transplantation. *Liver Transplantation* 16, 229–237.
- Tsang, T.H., Himmelblau, D.M., Edgar, T.F., 1975. Optimal control via collocation and non-linear programming. *International Journal of Control* 21, 763–768.
- Uhrig, M., Ezquer, F., Ezquer, M., 2022. Improving cell recovery: Freezing and thawing optimization of induced pluripotent stem cells. *Cells* 11, 799.
- Velardi, S.A., Barresi, A.A., 2008. Development of simplified models for the freeze-drying process and investigation of the optimal operating conditions. *Chemical Engineering Research and Design* 86, 9–22.
- Wächter, A., Biegler, L.T., 2006. On the implementation of an interior-point filter line-search algorithm for large-scale nonlinear programming. *Mathematical Programming* 106, 25–57.